Hydroperoxyl Radical Reactions. I. Electron Paramagnetic Resonance Study of the Complexation of $H\dot{O}_2$ with Some Metal Ions

D. Meisel,[1a] G. Czapski,*[1a] and A. Samuni[1b]

Contribution from the Department of Physical Chemistry, The Hebrew University, Jerusalem, Israel, and the Radiation Research Laboratories and Center for Special Studies, Mellon Institute of Science, Carnegie-Mellon University, Pittsburgh, Pennsylvania 15213. *Received January 23, 1973*

Abstract: Complexes of $H\dot{O}_2$ radical with the transition metal ions Th(IV), U(VI), Zr(IV), and Ti(IV) were generated in a flow system by mixing the corresponding metal ion either with $H\dot{O}_2$ or with $M\text{–}H\dot{O}_2$. The paramagnetic species were followed by epr spectroscopy. The results indicate that both the exchange reaction $M\text{–}H\dot{O}_2 + M' \rightleftharpoons M + M'\text{–}H\dot{O}_2$ (1) and the formation reaction $M + H\dot{O}_2 \rightleftharpoons M\text{–}H\dot{O}_2$ (2) are reversible fast processes. The mechanisms of these reactions were studied and the equilibria constants were determined. Values of $K_1 = (1.9 \pm 0.2) \times 10^{-2}$, $(1.8 \pm 0.2) \times 10^{1}$, and 3.6 ± 0.3 were determined for the couples Th(IV)–U(VI), U(VI)–Zr(IV), and Zr(IV)–Th(IV), respectively, and $K_2 = (2.7 \pm 0.4) \times 10^{3}$ and $(1.7 \pm 0.4) \times 10^{5}\ M^{-1}$ for M = U(VI) and Th(IV), respectively. Lower limits for the rate constants of these reactions were estimated. The decay of $M\text{–}H\dot{O}_2$ is shown to proceed through the free $H\dot{O}_2$ radical as well as through the complexed form. Rate constants for the various modes of decay reactions in the presence of M = Th(IV) and U(VI) were determined.

We have reported previously[2] that a reversible exchange reaction occurs where a peroxy radical is transferred between various transition metal ions according to

$$M\text{–}H\dot{O}_2 + M' \underset{k_{-1}}{\overset{k_1}{\rightleftharpoons}} M + M'\text{–}H\dot{O}_2 \qquad (1)$$

These complexes with $H\dot{O}_2$ ($M\text{–}H\dot{O}_2$) were shown[2–12] to be formed through the reactions of $H\dot{O}_2$ with the free metal ion in its highest stable oxidation state as well as *via* an oxidation of the metal–peroxy complexes by $H\dot{O}_2$ and/or $\dot{O}H$ radicals.[13] We extended this study to the kinetics of the formation and exchange reactions of the complexed radical. Although the over-all exchange reaction is represented in eq 1, the actual mechanism may proceed either directly or *via* the dissociation of the complex into the free $H\dot{O}_2$ according to the following reactions

$$M + H\dot{O}_2 \underset{k_{-2}}{\overset{k_2}{\rightleftharpoons}} M\text{–}H\dot{O}_2 \qquad (2)$$

$$M' + H\dot{O}_2 \underset{k_{-3}}{\overset{k_3}{\rightleftharpoons}} M'\text{–}H\dot{O}_2 \qquad (3)$$

In order to study the exchange reaction, we generated $H\dot{O}_2$ radicals through the instantaneous reduction of Ce(IV) by an excess of H_2O_2 in 0.1 M $HClO_4$[14]

$$\text{Ce(IV)} + H_2O_2 \xrightarrow{k_4} \text{Ce(III)} + H\dot{O}_2 + H^+ \qquad (4)$$

The $H\dot{O}_2$ formed in reaction 4 reacts through reactions 2 and 3 or decays *via* the self-recombination reaction 5. In the presence of metal ions the radicals decay mainly through additional modes which will be discussed.

$$H\dot{O}_2 + H\dot{O}_2 \xrightarrow{k_5} H_2O_2 + O_2 \qquad (5)$$

In this study $M\text{–}H\dot{O}_2$ and $H\dot{O}_2$ were generated in a flow system and their properties were studied using esr spectroscopy.

Experimental Section

Reagents. Thorium nitrate and uranyl nitrate (B.D.H. "Analar"), zirconium nitrate (Fisher Chemicals), B.D.H. 30% hydrogen peroxide, and Merck's 70% perchloric acid were used without further purification. Ceric perchlorate was prepared, stored, and its concentration was determined as previously described.[14] Titanic perchlorate was prepared from titanyl chloride as previously described.[15] All solutions were made up from triply distilled water and contained 0.1 M $HClO_4$.

Apparatus. The esr spectrometer, the flow system, and the experimental details have been described elsewhere.[9]

The mixing of the reactants was carried out by means of: (a) a standard Varian V 4549 liquid-flow-mixing cell; (b) a double-mixing cell formed by two joined mixing cells in series (with a dead volume of 1.7 cm^3 between first and second mixers); (c) a double-mixing cell with a dead volume of 0.03 ml between its mixers.

The dead volume between the last mixer and the middle of the observation cell was 0.15 cm^3. The time intervals between mixing and observation or between the two mixing stages were controlled by either varying the dead volumes or changing the flow rate. Flow rates ranged from 1 up to 10 cm^3/sec. The introduction of the various reactants into the reaction mixture, using either simple or double-mixing cells, is given schematically in Figure 1. When the double-mixing cell was used (Figure 1), special care was taken to ensure that no detectable free $H\dot{O}_2$ would find its way to the second mixing cell. (This was checked by introducing a large

---

[1] (a) The Hebrew University; (b) Carnegie–Mellon University.

[2] A. Samuni and G. Czapski, *J. Phys. Chem.*, **74**, 4592 (1970).

[3] W. T. Dixon and R. O. C. Norman, *Nature (London)*, **196**, 891 (1962).

[4] (a) V. H. Fischer, *Ber. Bunsenges. Phys. Chem.*, **71**, 685 (1967); (b) M. S. Bains, J. C. Arthur, and O. Hinojosa, *ibid.*, **72**, 2250 (1968).

[5] V. F. Shuvalov and N. M. Bazhin, *Zh. Strukt. Khim.*, **10**, 548 (1969).

[6] M. Setaka, Y. Kirino, T. Ozawa, and T. Kwan, *J. Catal.*, **15**, 209 (1969).

[7] M. S. Bains, J. C. Arthur, and O. Hinojosa, *J. Amer. Chem. Soc.*, **91**, 4673 (1969).

[8] A. Samuni and G. Czapski, *Isr. J. Chem.*, **8**, 563 (1970).

[9] G. Czapski, H. Levanon, and A. Samuni, *ibid.*, **7**, 375 (1969).

[10] A. P. Mezkulov, N. M. Bazhin, and V. M. Berdnikov, *Zh. Strukt. Khim.*, **11**, 1121 (1970).

[11] M. S. Bains, J. C. Arthur, Jr., and O. Hinojosa, *Inorg. Chem.*, **9**, 1570 (1970).

[12] Y. Shimizo, T. Shiga, and K. Kuwata, *J. Phys. Chem.*, **74**, 2929 (1970).

[13] A. Samuni, *J. Phys. Chem.*, **76**, 2207 (1972).

[14] G. Czapski and A. Samuni, *Isr. J. Chem.*, **7**, 361 (1969).

[15] V. Krishnan and C. C. Patel, *Chem. Ind. Int.*, 321 (1961).

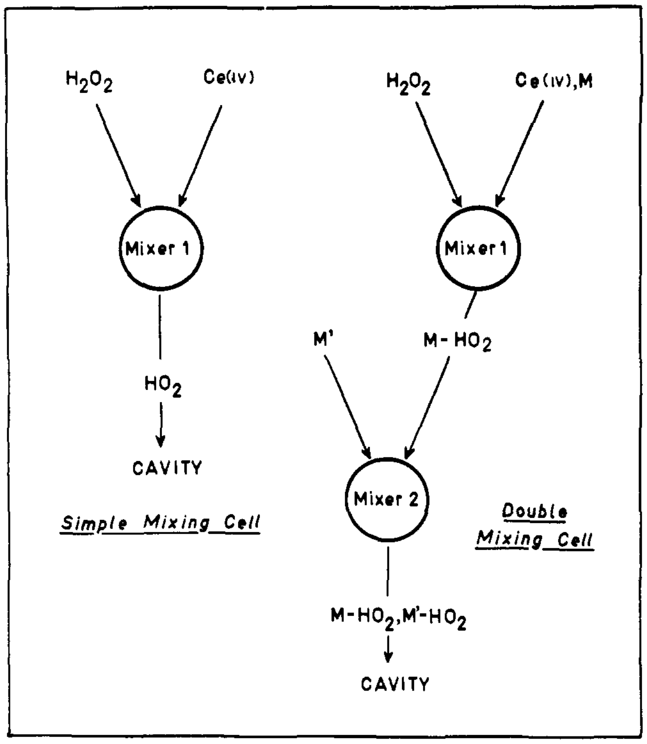

Figure 1. The different mixing cells (and mixing procedures) are shown schematically. Each circle represents a mixer having four jets used for mixing two solutions.

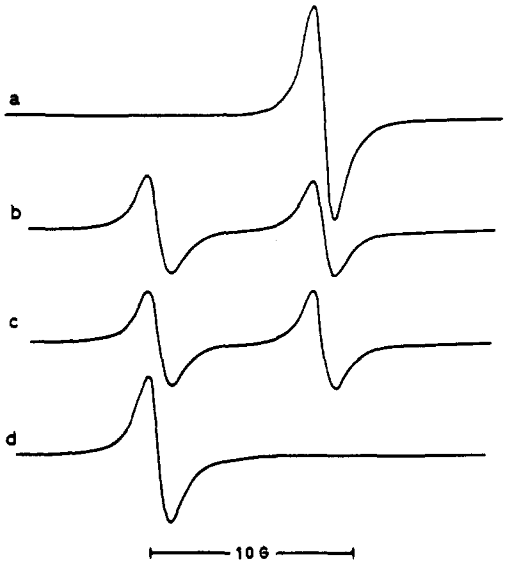

Figure 2. Esr spectra obtained on mixing Ce(IV) (0.1 m*M*) with H_2O_2 (2 m*M*) in mixer 1 of a double-mixing cell where the resulting mixture was mixed thereafter again with 2 m*M* H_2O_2 in mixer 2. Metal ions were introduced into the system in the following order: (a) 0.4 m*M* Th(IV) at mixer 1; (b) 0.4 m*M* Th(IV) and 25 m*M* U(VI) at mixer 1 and mixer 2, respectively; (c) 0.4 m*M* Th(IV) and 25 m*M* U(VI) at mixer 2 and mixer 1, respectively; (d) 25 m *M* U(VI) at mixer 1.

Table I. Dependence of Th–$H\dot{O}_2$ and U–$H\dot{O}_2$ Signal Intensities on [U(VI)][a]

[U(VI)],[b] m*M*	Relative intensity [Th–$H\dot{O}_2$]	[U–HO_2]	[Th(IV)][U–$H\dot{O}_2$]/[U(VI)][Th–$H\dot{O}_2$]
0	106	0	
0.67	93	6.2	1.8×10^{-2}
1.3	87	12	1.9×10^{-2}
3.8	69	26	1.8×10^{-2}
6.7	55	37	1.8×10^{-2}
10.2	42	46	1.9×10^{-2}
17	29	54	2.0×10^{-2}
28	19	58	2.0×10^{-2}

[a] Obtained on mixing 0.1 *M* H_2O_2 with 0.036 m*M* Ce(IV) and 0.55 m*M* Th(IV) at the first mixing point and various concentrations of U(VI) at the second mixing point. All solutions in 0.1 *M* $HClO_4$. [b] Final concentration of U(VI) in the cavity. [Th(IV)] in the cavity is 0.18 m*M* due to dilution.

excess of Th(IV) at mixer 2. In such a case, even traces of $H\dot{O}_2$ radical arriving from mixer 1 would react with Th(IV), yielding the easily detectable, long-lived Th(IV)–$H\dot{O}_2$ radicals.) All concentrations of the reactants were corrected, according to the corresponding dilution due to mixing. All experiments were carried out at ambient temperature (22 ± 3°). Relative intensities of the esr signals were taken as proportional to $(\Delta H)^2h$, where ΔH is the peak-to-peak separation in the first derivative curve, and h is the peak-to-peak height of the signal. Where absolute concentrations of the paramagnetic species were calculated, the areas under absorption curves were calibrated using solutions of $VOSO_4$. To minimize the errors due to possible small changes in the cell location upon changing the sample, the cell was placed in a fixed position inside the cavity; the solutions were changed without removing the cell. Care was taken to keep all settings of the spectrometer knobs unchanged except for the recorder attenuation within a given series of experiments. When intensities of signals with different width were compared, the changes due to different modulation amplitude and microwave power were corrected for, using a standard solution of $VOSO_4$. Special care was taken to avoid saturation of any of the signals.

Results and Discussion

Exchange Reaction. Reaction 1 was investigated by following the esr spectra of Th(IV)–$H\dot{O}_2$ and U(VI)–$H\dot{O}_2$, denoted as M–$H\dot{O}_2$ and M′–$H\dot{O}_2$, respectively, obtained on reacting Th(IV)–$H\dot{O}_2$ radicals with U(VI) ions. M–$H\dot{O}_2$ radicals were produced from Ce(IV) + M + H_2O_2 at mixer 1 while M′–$H\dot{O}_2$ formed on introducing solutions of M′ ions at mixer 2 (see Figure 1). Then the order of mixing was reversed; *i.e.*, U(VI) has been premixed with the Ce(IV) ions while Th(IV) solution was introduced at mixer 2. The obtained spectra are displayed in Figure 2. This experiment was repeated varying the concentration of M′ and keeping [M] constant. In Table I the relative intensities of both M–$H\dot{O}_2$ and M′–$H\dot{O}_2$ are described as a function of [M′] (at a constant [M]). It is seen in Table I that [M–$H\dot{O}_2$] decreases on increasing [M′] while [M′–$H\dot{O}_2$] increases correspondingly. The total concentration of the complexed paramagnetic species is slightly reduced on increasing [U(VI)] as a result of the faster decay rate of its complex. This effect will be discussed later. The results were identical when the roles of the metal ions M and M′ were reversed. In this case M–$H\dot{O}_2$ signal increased on the account of M′–$H\dot{O}_2$ as more M ions were added (keeping [M′] constant).

In all our experiments, unless otherwise stated, [M] and [M′] were kept high enough as compared to [Ce(IV)]$_0$ = [$H\dot{O}_2$]$_0$; thus changes in the metal ion concentration due to the formation of M–$H\dot{O}_2$ and M′–$H\dot{O}_2$ were negligible. These results indicate that equilibrium 1, as previously reported,[2] does exist. In order to find out whether equilibrium 1 is already achieved at the observation point, the ratio [M′$H\dot{O}_2$][M]/[M$H\dot{O}_2$]·[M′] was calculated and is given in Table I. In the case where the equilibrium reaction 1 is slow, a relatively high concentration of the metal should be used; otherwise the value of this ratio would not equal K_1. If

Table II. Equilibrium Constant for the Reaction $M\text{-}H\dot{O}_2 + M' \rightleftharpoons M + M'\text{-}H\dot{O}_2$

M	M′	K_1	k_1, M^{-1} sec^{-1}	k_{-1}, M^{-1} sec^{-1}
Th(IV)	U(VI)	$(1.9 \pm 0.2) \times 10^{-2}$	$\geqslant 1.2 \times 10^3$	$\geqslant 7.2 \times 10^4$
U(VI)	Zr(IV)	$(1.8 \pm 0.2) \times 10^1$		
Zr(IV)	Th(IV)	3.6 ± 0.3	$\geqslant 1.4 \times 10^4$	$\geqslant 4 \times 10^3$

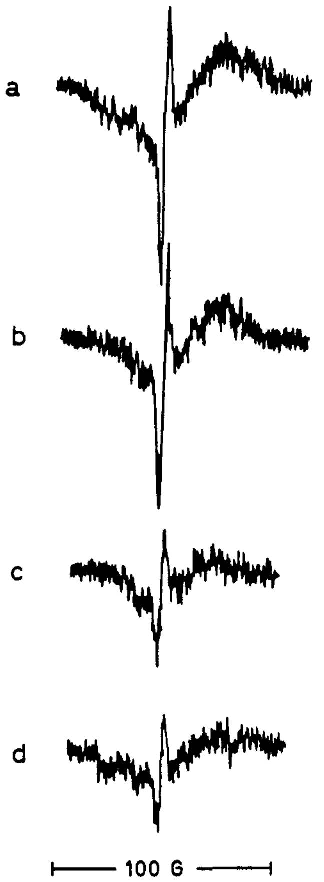

Figure 3. Superposition of the esr signals of $H\dot{O}_2$ and $M\text{-}H\dot{O}_2$ obtained on recording the flowing reaction mixture of 0.1 mM Ce(IV), 2.5 mM H_2O_2, and 0.017 mM U(VI) at the following flow rates: (a) 8, (b) 7, (c) 2, and (d) 1.7 cm^3/sec.

equilibrium 1 is obtained, no dependence on [M′] is expected and the equilibrium constant can be determined from the expression

$$K_1 = \frac{[M'\text{-}H\dot{O}_2][M]}{[M\text{-}H\dot{O}_2][M']} \qquad (6)$$

As seen in Table I this is the case under the present experimental conditions. No dependence on [M′] nor on the order of introducing the two cations is observed even at the low concentrations of the metal ion, thus indicating that the equilibrium is already achieved at the detection point. From the lowest [M] at which the observed value of $[M'\text{-}H\dot{O}_2][M]/[M\text{-}H\dot{O}_2][M']$ was equal to K_1 at ~50 msec after the second mixing, a lower limit for k_1 and k_{-1} can be estimated.

We have repeated these experiments replacing Th(IV) and U(VI) by the couples U(VI)–Zr(IV) and Zr(IV)–Th(IV). Similar results were obtained. The equilibrium constants were calculated using expression 6 and are summarized in Table II along with the lower limit estimation for its rate constants. Further support for these calculated values was obtained by multiplying the corresponding constants $K_{\text{Th-U}} \times K_{\text{U-Zr}} \times K_{\text{Zr-Th}}$. The obtained value is 1.04 which is very close to unity as expected.

Although these results proved the existence of fast equilibria (within less than 50 msec), they do not enable us to distinguish between the possible mechanism (*i.e.*, reaction 1 or reactions 2 and 3) by which the equilibrium is achieved. This question will be discussed further on.

When Ce(IV) was mixed with Ti(IV) + H_2O_2, at the first mixer, the two well-known singlets[4a] (usually denoted S_1 and S_2) were observed. These signals were previously attributed to different Ti(IV)–$H\dot{O}_2$ complexes.[4a] On addition of Th(IV) at the second mixing point, to solutions containing S_1 and S_2, no signal due to Th–$H\dot{O}_2$ could be detected. This seems to indicate that K_2 for Ti(IV) is very high and k_{-2} is rather slow. Fischer's[4a] observation that S_1 and S_2 decay at different rates is in accord with this result, since this indicates that S_1 and S_2 are not at equilibrium with each other.

Formation Reaction of $M\text{-}H\dot{O}_2$ Radical. The esr spectrum obtained on adding low concentrations of M ions to the reaction mixture of H_2O_2 + Ce(IV) consists of a narrow signal (~1 G) due to $M\text{-}H\dot{O}_2$ radical[2] superimposed on the $H\dot{O}_2$ broad signal[16] (~27 G), as shown in Figure 3. Three assumptions might be made regarding the coexistence of these two forms of the radical ($H\dot{O}_2$ and $M\text{-}H\dot{O}_2$).

I. A fast equilibrium between the free and the complexed radical exists. In such a case, the concentration ratios of the two forms should be independent of the time interval between mixing and observation points. The equilibrium constant might then be calculated from

$$K_2 = k_2/k_{-2} = [M\text{-}H\dot{O}_2]/[H\dot{O}_2][M] \qquad (7)$$

II. An alternative assumption might be that the reaction of $H\dot{O}_2$ with M yields $M\text{-}H\dot{O}_2$, which does not dissociate. In this case, Figure 3 describes a situation where reactions 2 and 5 are in competition. According to this mechanism, $k_{-2} = 0$ while k_2 can be determined by means of a scavenging curve. In such a case, increasing the flow rate would result in a decrease of $[M\text{-}H\dot{O}_2]/[H\dot{O}_2]$ ratio.

III. The third possibility is the existence of a reversible reaction[2,3] which is slow; therefore, reactions 2, −2, and 5 compete.

To ascertain the true mechanism, we investigated the influence of the variation of the flow rate (all other factors are constant) on $[M\text{-}H\dot{O}_2]/[H\dot{O}_2]$. On using a standard Varian mixing cell we changed the flow rate from 1 up to 10 cm^3/sec. Thus we varied the time interval between mixing and observation from 150 to 15 msec (in this time range the total radicals' concentration change is by a factor of 2.5) and measured the relative intensities of $H\dot{O}_2$ and $M\text{-}H\dot{O}_2$ esr signals. From

---

(16) E. Saito and B. H. J. Bielski, *J. Amer. Chem. Soc.*, 83, 4467 (1961).

Figure 3 it is seen that, within the experimental error, the ratio $[\mathrm{M{-}H\dot{O}_2}]/[\mathrm{H\dot{O}_2}]$ was time independent. Hence it indicates that a fast equilibrium is maintained between the complexed and the "naked" forms of the hydroperoxyl radical. This suggests that assumption I and not II or III is valid. The fast exchange of the peroxyl radical between M and M′ may thus proceed *via* reactions 2 and 3, but one cannot exclude the possibility that a direct exchange takes place (reaction 1).

In order to determine the equilibrium constant K_2, the set of experiments described in Figure 3 was repeated. Ce(IV) (0.1 m*M*) was mixed with 5 m*M* $\mathrm{H_2O_2}$ in the presence of either Th(IV) or U(VI) ions. The relative intensities of the two superimposed signals were determined separately from the areas under the respective absorption curves. Since the esr signals of $\mathrm{M{-}H\dot{O}_2}$ and $\mathrm{H\dot{O}_2}$ differ markedly in their widths ($\sim$1 and $\sim$27 G, respectively), the narrow line was quickly saturated under the experimental conditions in which the broad one was observed. This made it necessary to measure them separately, each at the appropriate modulation amplitude and microwave power. The results are shown in Table III. In order to observe both $\mathrm{M{-}H\dot{O}_2}$ and $\mathrm{H\dot{O}_2}$ simultaneously, the concentration of the metal ion had to be reduced in these experiments to concentrations not much higher than $[\mathrm{M{-}H\dot{O}_2}]$. In such cases [M] was corrected for the amount of the complexed metal, assuming a ratio of 1:1 in $\mathrm{M/H\dot{O}_2}$ in the complex. The values of K_2 determined by this method are liable to quite a large experimental error since the signal of the complex tended to overlap somewhat the $\mathrm{H\dot{O}_2}$ signal. From the values shown in Table III, at maximal flow rate and lowest [M], we could estimate lower limits for the rate constants of reactions 2 and -2 for both Th(IV) and U(VI). The values thus obtained are given in Table III. Taking these lower limits of k_2 and k_{-2} for Th(IV) and U(VI), we find, by numerically integrating the corresponding rate equations, that the half-life time for the achievement of equilibrium 1, at the conditions of Table I, is less than 20 msec. We conclude therefore that reactions 2 and -2 are fast enough to ensure that equilibrium 1 is reached. Yet the possibility of direct exchange cannot be discarded if k_1 and k_{-1} are much larger than our lower limit values.

Table III. Relative Intensities of $\mathrm{H\dot{O}_2}$ and $\mathrm{M{-}H\dot{O}_2}$ in the Reaction Mixture of Ce(IV) + $\mathrm{H_2O_2}$ + M

	[M],[a] μM	Flow rate, cm^3/sec	Relative intensity[b] $\mathrm{H\dot{O}_2}$	Relative intensity[b] $\mathrm{MH\dot{O}_2}$	$K_2 = [\mathrm{M{-}H\dot{O}_2}]/[\mathrm{H\dot{O}_2}][\mathrm{M}]$, M^{-1}
M = U(VI)	13	2.5	515	20	3.0×10^3
	13	4.5	850	30	2.7×10^3
	25	2.6	600	35	2.3×10^3
	25	4.5	880	62	2.8×10^3
			$k_2 \geqslant 1 \times 10^5\ M^{-1}\ \mathrm{sec}^{-1}$	$k_{-2} \geqslant 40\ \mathrm{sec}^{-1}$	$\bar{K}_2 = (2.7 \pm 0.4) \times 10^3$
M = Th(IV)	2.9	3.6	145	76	1.8×10^5
	5.2	5.0	410	300	1.4×10^5
	5.7	1.8	115	130	2.0×10^5
			$k_2 \geqslant 5 \times 10^6\ M^{-1}\ \mathrm{sec}^{-1}$	$k_{-2} \geqslant 30\ \mathrm{sec}^{-1}$	$\bar{K}_2 = (1.7 \pm 0.4) \times 10^5$

[a] Corrected for the complexed metal ion concentration. All solutions are in 0.1 *M* $\mathrm{HClO_4}$. [b] Relative intensities of $\mathrm{H\dot{O}_2}$ and $\mathrm{MH\dot{O}_2}$ were measured at different modulation amplitudes and microwave power. The calibration was done using $\mathrm{VOSO_4}$ solutions under the respective conditions.

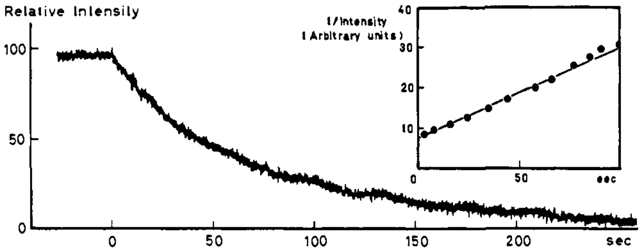

Figure 4. Decay curve of the Th–$\mathrm{H\dot{O}_2}$ radical and the second-order criterion for this decay (insert): obtained on mixing 0.1 m*M* Ce(IV) with 0.1 *M* $\mathrm{H_2O_2}$ containing 3.5 m*M* Th(IV).

The assumption that equilibria 2 are achieved under the conditions given in Table III gets further support when comparing the ratio $K_{2\mathrm{U(VI)}}/K_{2\mathrm{Th(IV)}}$ with K_1 for this couple of metal ions, as obtained independently in Table II. This ratio turns out to be 1.6×10^{-2}, practically equal, within experimental error, to $K_1 = 1.9 \times 10^{-2}$, as would be expected. We believe, therefore, that the apparent trend in K_2 for Th(IV) is within the range of experimental error.

Decay Kinetics of $\mathrm{M{-}H\dot{O}_2}$. It has been shown previously[2] that in most cases $\mathrm{M{-}H\dot{O}_2}$ decays slower than the free $\mathrm{H\dot{O}_2}$. Since equilibrium 2 is reached very fast compared with the slow decay of $\mathrm{M{-}H\dot{O}_2}$, its decay might reflect the decay of $\mathrm{H\dot{O}_2}$ through reaction 5. If reaction 5 is the only pathway through which $\mathrm{M{-}H\dot{O}_2}$ decays, we would expect an increase in $\tau_{1/2}$ on increasing [M]. The effect of [M] on $\tau_{1/2}$ of $\mathrm{M{-}H\dot{O}_2}$ was studied, using the stopped-flow technique. In this set of experiments solutions of 0.1 m*M* Ce(IV) were mixed with 0.1 *M* $\mathrm{H_2O_2}$ containing increasing amounts of [M]. The magnetic field was set at the peak of the $\mathrm{M{-}H\dot{O}_2}$ line, and the decrease in signal intensity, after quickly stopping the reaction's mixture flow, was followed. In all experiments decay curves similar to those displayed in Figure 4 were obtained. In all cases the response time of the detecting and recording set up was at least an order of magnitude less than $\tau_{1/2}$ of the chemical reaction. Table IV summarizes the effect of [M] on the decay rate of $\mathrm{M{-}H\dot{O}_2}$, for M = Th(IV), U(VI), and mixtures of both metal ions. The decay was always second order and the rate is seen to decrease on increasing [Th(IV)] or [U(VI)]. The uranyl complex disappears faster than the thorium complex in reaction mixtures in which $[\mathrm{H\dot{O}_2}]_{\mathrm{free}}$ (uncomplexed $\mathrm{H\dot{O}_2}$) is comparable. Furthermore, addition of U(VI) to solutions containing Th(IV) decreases considerably $\tau_{1/2}$ of the decay of both complexes. In the latter case both Th–$\mathrm{H\dot{O}_2}$ and U–$\mathrm{H\dot{O}_2}$ decay at the same rate.

This confirms the existence of the fast equilibrium 1, as compared with the slow decay of $\mathrm{M{-}H\dot{O}_2}$. Furthermore, these results indicate that in addition to the self-recombination reaction (reaction 5), $\mathrm{M{-}H\dot{O}_2}$ decays also through the other second-order processes, reaction 8 and possibly through reaction 9. If $k_5 > k_8, k_9$,

$$\mathrm{M{-}HO_2 + HO_2 \longrightarrow M + H_2O_2 + O_2} \tag{8}$$

$$\mathrm{M{-}HO_2 + M{-}HO_2 \longrightarrow 2M + H_2O_2 + O_2} \tag{9}$$

Table IV. Decay Kinetics of M–$H\dot{O}_2$[a]

[Th(IV)], mM	[U(VI)], mM	$\tau_{1/2}$, sec[b]	$2k_{obsd}$[c] × 10^{-4}, M^{-1} sec^{-1}	[Th(IV)], mM	[U(VI)], mM	$\tau_{1/2}$, sec[b]	$2k_{obsd}$[c] × 10^{-5}, M^{-1} sec^{-1}
0.25		5.5	4.9		1.25	0.47	8.1
0.55		14	2.2		2.65	0.78	4.4
0.90		18	1.4		4.1	0.96	2.4
1.30		27	0.8		7.2	1.10	1.7
1.75		37	0.7		10.30	1.30	1.4
2.25		50	0.4		13.60	1.45	1.1
4.05		70	0.3		21.00	1.55	1.0
4.05	4.65	34	0.5		27.60	1.70	0.95
4.05	11.50	17	1.1	0.45	27.60	2.10	0.8
				0.90	27.60	2.80	0.8
				2.10	27.60	4.20	1.0
				3.50	27.60	6.40	7.0

[a] Mixing 0.1 mM Ce(IV) with 0.1 M H_2O_2 + M solutions, all at 0.1 M $HClO_4$. [b] Half-life time of M–$H\dot{O}_2$ decay. In cases of mixtures of M–$H\dot{O}_2$ both radicals decay at the same rate. [c] $2k_{obsd} = d(1/[M\text{–}H\dot{O}_2])/dt$.

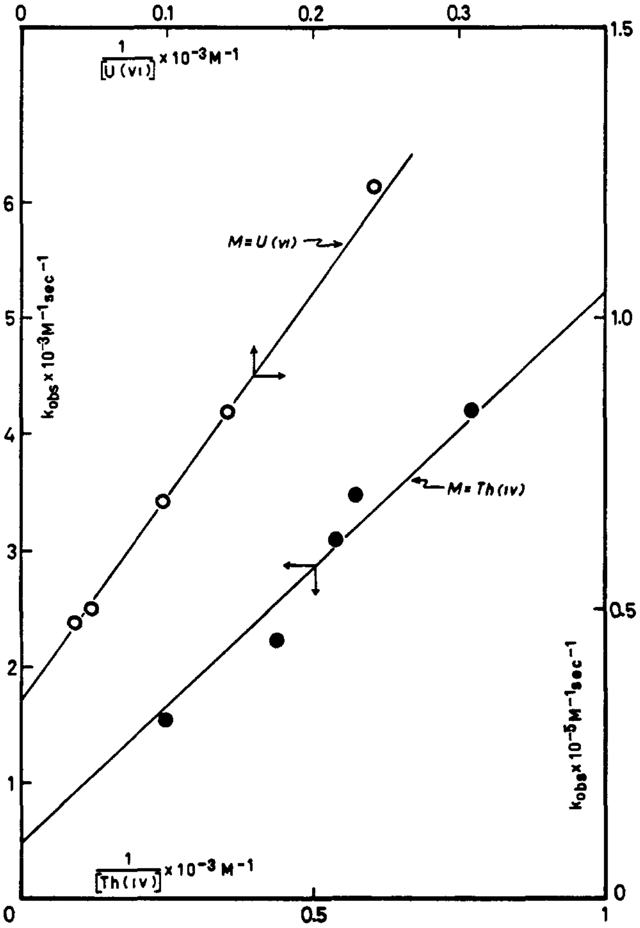

Figure 5. The dependence of k_{obsd} on 1/[M]: (●) = Th(IV), (○) M = U(VI).

then the increase in $\tau_{1/2}$ of the radical's decay, on increasing [M], is attributable to the replacement of the relatively fast decaying $H\dot{O}_2$ radicals by the less reactive M–$H\dot{O}_2$ radicals. The above reaction scheme (reactions 2, 5, 8, and 9) would imply the following rate law.

$$-\frac{d[HO_2]_{total}}{dt} = 2k_5[H\dot{O}_2]_{free}^2 + 2k_8[M\text{–}H\dot{O}_2][H\dot{O}_2]_{free} + 2k_9[M\text{–}H\dot{O}_2]^2 = 2k_{obsd}[H\dot{O}_2]_{total}^2 \quad (10)$$

where

$$[H\dot{O}_2]_{total} = [H\dot{O}_2]_{free} + [M\text{–}H\dot{O}_2] \quad (11)$$

Since equilibrium 2 is achieved quickly compared with the decay of M–$H\dot{O}_2$, we can assume

$$[H\dot{O}_2]_{free} = [H\dot{O}_2]_{total}/(1 + K_2[M]) \quad (12)$$

The observed rate constant, k_{obsd}, would then be given by eq 13. Integrating the rate equation 10 and sub-

$$k_{obsd} = \frac{k_5 + k_8K_2[M] + k_9K_2^2[M]^2}{(1 + K_2[M])^2} \quad (13)$$

stituting $[HO_2]_{total}$ and $[HO_2]_{free}$ from eq 11 and 12, one gets

$$[M\text{–}H\dot{O}_2] = \frac{K_2[M][H\dot{O}_2]_0(1 + K_2[M])}{(1 + K_2[M])^2 + 2(k_5 + k_8K_2[M] + k_9K_2^2[M]^2)[H\dot{O}_2]_0t} \quad (14)$$

The second-order criterion would then take the form

$$\frac{1}{[M\text{–}H\dot{O}_2]} = \frac{1 + K_2[M]}{K_2[M][HO_2]_0} + \frac{2k_{obsd}(1 + K_2[M])t}{K_2[M]} \quad (15)$$

Indeed the M–$H\dot{O}_2$ decay followed the second-order criterion for at least 70% of the reaction, as can be seen in the example inserted in Figure 4. For the range of [M], where most $H\dot{O}_2$ radicals are complexed, $K_2[M] > 1$, the slopes of such curves are equal to $2k_{obsd}$, and k_{obsd} reduces to

$$k_{obsd} = k_9 + \frac{k_8}{K_2[M]} + \frac{k_5}{(K_2[M])^2} \quad (16)$$

If the last term in eq 16 is negligible as compared with the other terms, *i.e.*, the decay through free $H\dot{O}_2$ may be neglected, k_{obsd} should depend linearly on 1/[M]. This turns out to be the case for the higher range of [M] as is shown in Figure 5. From the slopes of this figure and the values of K_2 determined in Table III, we get k_8 = (8.0 ± 2.0) × 10^5 M^{-1} sec^{-1} for Th–$H\dot{O}_2$ and k_8 = (9.0 ± 1.5) × 10^5 M^{-1} sec^{-1} for U–$H\dot{O}_2$. From the intercepts of this figure, we get k_9 = (5 ± 2) × 10^2 M^{-1} sec^{-1} and k_9 = (4 ± 1) × 10^4 M^{-1} sec^{-1} for Th(IV) and U(VI), respectively.

Obviously, even at concentrations of Th(IV) where $[H\dot{O}_2]_{free}$ amounts only to ~1% of $[H\dot{O}_2]_{total}$, the complex Th–H$\dot{O}_2$ decays mainly through reaction 8 while the U–H$\dot{O}_2$ decays mainly through reaction 9 at much higher $[H\dot{O}_2]_{free}/[U\text{–}H\dot{O}_2]$ ratios.

Equation 14 provides an explicit relation between [M] and the generated [M–H$\dot{O}_2$]. In order to check the validity of these assumptions we mixed a solution of 0.05 m*M* Ce(IV) with 0.1 *M* H_2O_2, using a single mixing cell at a constant flow rate (1.6 cm^3/sec). Th(IV) ions were added either to the Ce(IV) or to the H_2O_2 solution and the relative intensities of the Th–H$\dot{O}_2$ esr signals observed were recorded. The results are shown in Figure 6 where [Th–H$\dot{O}_2$] is plotted *vs.* [Th(IV)]. The same set of experiments was then repeated, varying *t* by changing the "dead volume." These results are represented by the family of curves (each for a certain *t*) which at high [M] approach the plateau value which corresponds to

$$[M\text{–}H\dot{O}_2]_{\text{at the plateau}} = [H\dot{O}_2]_0 = [\text{Ce(IV)}]_0 \qquad (17)$$

Using expression 14 we could evaluate K_2, k_8, and k_9, taking $k_5 = 7.5 \times 10^5\ M^{-1}\ \text{sec}^{-1}$ [17] and *t* from the flow rate and the dead volume and $[HO_2]_0$ from eq 17. This was carried out using a nonlinear least-squares method, and the obtained values were used to plot the solid lines in Figure 6. The computed curves agree quite well with the measured values. Although this method is a rather poor way for quantitative determination of these parameters, it can provide useful information regarding their order of magnitude. The values ($K_2 = 2.3 \times 10^5$; $k_8 = 9.5 \times 10^5\ M^{-1}\ \text{sec}^{-1}$; $k_9 = 150\ M^{-1}\ \text{sec}^{-1}$) thus achieved might be compared with those determined directly (Table III and Figure 5).

K_2 and k_8 thus obtained agree with the direct determination within 20% while k_9 differs by a factor of ~3. Both determinations are very inaccurate regarding k_9, as the contribution of reaction 9 is rather small.

Conclusions

We can now summarize the above-mentioned results as follows.

H$\dot{O}_2$ radicals react with metal ions yielding complexed radicals.

The complexation reaction is reversible, and a fast equilibrium is achieved, even at very low concentrations of the metal ions.

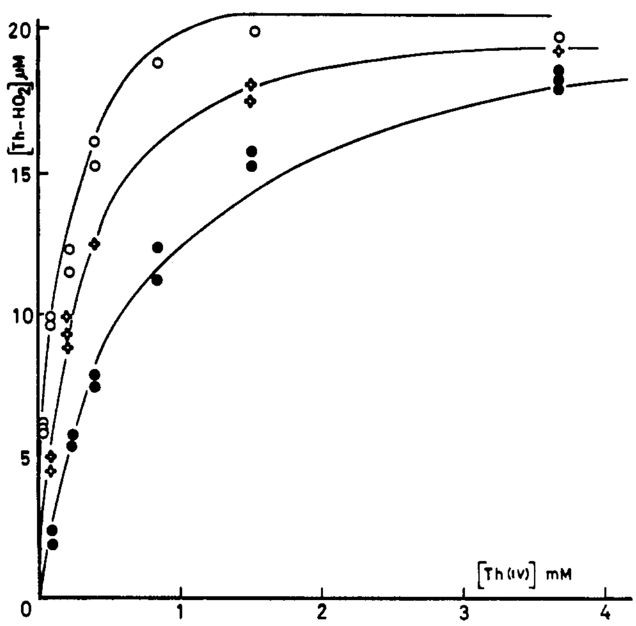

Figure 6. The relative intensity of the M–H$\dot{O}_2$ esr signal obtained on mixing 0.1 *M* H_2O_2 with 0.05 m*M* Ce(IV) in the presence of various concentrations of M ions at a flow rate of 1.6 cm^3/sec using different "dead-volumes" between mixing to observation: (a) 2.75, (b) 10.2, and (c) 25.0 cm^3.

The exchange of the peroxyl radical among various metal ions probably proceeds *via* the free H$\dot{O}_2$ radical, although the possibility of a direct exchange (reaction 1) cannot be excluded.

The formation of the complexed radical results in an apparent decrease of the decay rate of the radicals, due to a decrease in the effective concentration of the free H$\dot{O}_2$ radicals.

Both the self-recombination of H$\dot{O}_2$ and M–H$\dot{O}_2$ and the cross reaction of HO_2 with M–H$\dot{O}_2$ contribute to the decay of the radicals, where the relative contribution of these reactions depends on the metal ion and its concentration.

Acknowledgment. We gratefully acknowledge the support of this study by the U. S. Atomic Energy Commission under Contract AT(11-1)-3221 and AT(11-1)-3238.

---

[17] D. Behar, G. Czapski, J. Rabani, L. M. Dorfman, and H. A. Schwarz, *J. Phys. Chem.*, 74, 3209 (1970).